

3-D QSAR CoMFA Models of Pyrrolidine carboxamides for Prediction of Enoyl acyl carrier protein reductase Inhibitory Activity

Uday Chandra Kumar* and Mahmood Shaik

Bioinformatics Division, Environmental Microbiology Lab, Department of Botany, Osmania University, Hyderabad 500 007, A.P., India

*Address correspondence to:

E-mail address: dr.udaynair16@gmail.com

Abstract: Enoyl acyl carrier protein reductase is one of the key enzymes involved in the type II fatty acid biosynthesis pathway of *M. tuberculosis*. CoMFA analysis was performed using the molecular modeling package SYBYL 6.7.1 on silicon graphics work-station. A dataset of 46 Pyrrolidine carboxamide analogues reported to have Enoyl acyl carrier protein reductase inhibitory activities were used for the following QSAR studies. The CoMFA models yielded a good cross-validated correlation coefficient with LOO of 0.777 and with leave-many-out (q^2 with 10 groups) was 0.751, thus the predictions obtained with these models were reliable. The conventional correlation coefficient, r^2 between the actual and estimated activities of the molecules was observed as 0.966, using this model. The test set compatibility was substantiated by the r^2 pred value of 0.893. From QSAR studies the results have shown that Pyrrolidine carboxamide derivatives were proved to be highly potent inhibitors against *Mycobacterium tuberculosis* enoyl acyl carrier protein reductase.

Keywords: Comparative Molecular Field Analysis; 3D-QSAR; Pyrrolidine carboxamide; Enoyl acyl carrier protein reductase; *Mycobacterium tuberculosis*

Introduction

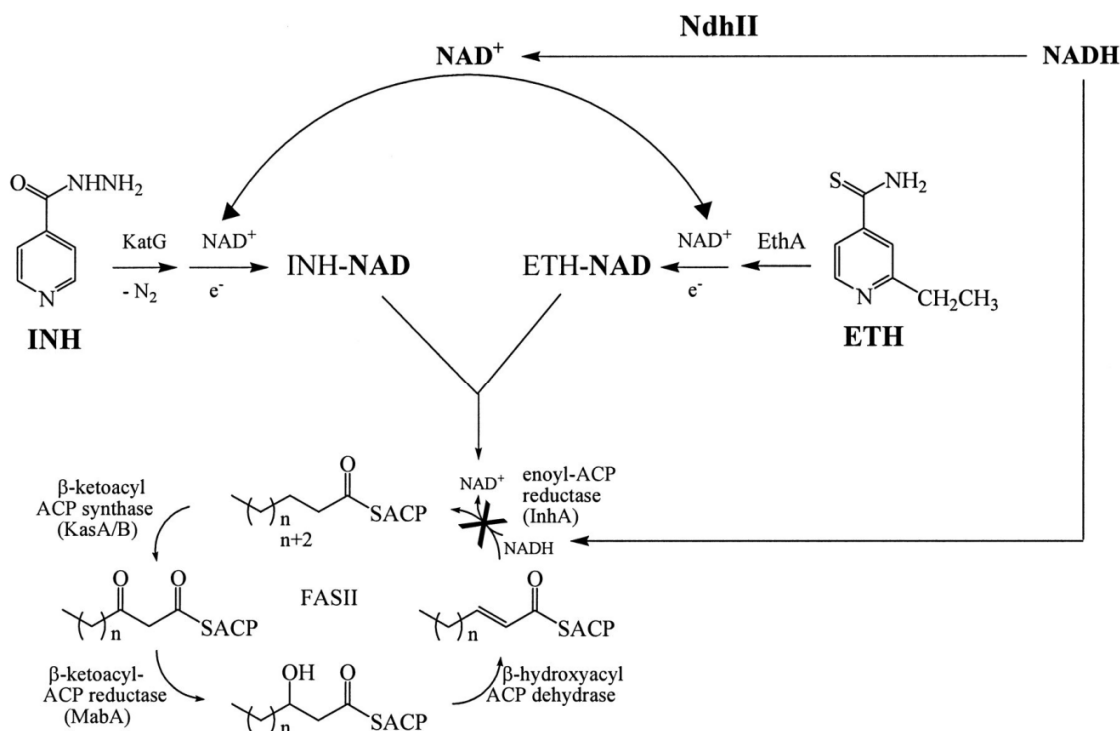
People more than 1.6 million per year were reported to have died due to Tuberculosis (TB) and about 8.8 million new cases are reported every year. Such a big number of people affected by TB indicate this disease as the most dangerous and fatal infectious disease. TB is overpowered by only AIDS among the infectious diseases. According to the data collected by World Health Organization, people suffering from multi-drug-resistance and extensively drug-resistant TB are increasing with at least a half million new cases being reported every year. Therefore, it has become necessary for the researchers to synthesize novel TB drugs (1).

The chronic infectious disease tuberculosis is caused by *Mycobacterium* species of the 'tuberculosis complex', which include *Mycobacterium bovis*, *Mycobacterium africanum*, and mainly *Mycobacterium tuberculosis*. Compared to other infectious diseases, TB has become more fatal to many adults. Isoniazid is known to be effective drug against TB when used in combination with other anti-TB drugs. Serious conditions like multi-drug resistant TB (MDR-TB) and extensively drug resistant TB (XDR-TB) are unsolved public health problems now (2–7).

Isoniazid (isonicotinic acid hydrazide, INH) which was discovered in 1952 is accepted now as the most important drug for the treatment of TB. It is a pro-drug which is processed later during metabolic oxidation by the *M. tuberculosis* enzyme, catalase-peroxidase katG (5, 8, and 9).

Mechanism

The INH-NAD(P) adducts were known to play role in preventing the action of the two enzymes called NAD-dependent enoyl-acyl carrier protein reductase (enoyl-ACP reductase, InhA) and NAD(P)-dependent beta-keto-ACP reductase (Mycolic acid biosynthesis A, MabA) which are involved in the fatty acid biosynthetic pathway of *M. tuberculosis* (10–13, 14).



Mechanism of action of INH and ETH.

The pro-drugs INH and ETH are triggered by the Catalase-Peroxidase KatG or the monooxygenase EthA, respectively. The activated forms react with NAD^+ to form an INH-NAD or ETH-NAD adduct. The enzymes InhA and NADH-dependent enoyl-ACP reductase of the fatty acid synthase type II system are inhibited by these two adducts which leads to the inhibition of mycolic acid biosynthesis and cell lysis. The stimulators of INH and ETH drugs are katG and ethA respectively. Recessive mutations in the katG and ethA genes create resistance to INH or ETH by stopping the activation of the drugs. Creating dominant mutation in the common target enzyme InhA, can induce co-resistance to INH and ETH drugs. This mutation will lead to a change in the target enzyme integrity. The Ndh enzyme is involved in increasing the intracellular concentration of NADH. Recessive mutations in Ndh gene will cause drug resistance by inhibiting competitively the association of INH-NAD or ETH-NAD adduct with InhA. This is a novel mechanism of co-resistance to INH and ETH (15).

In the current methods of treatment, the pro-drug isoniazid (INH) was found to destroy the bacterial cell wall by inhibiting the mycolic acid synthesis which is the significant constituent of integrated cell wall. (16). INH stimulated by KatG, a catalase-peroxidase enzyme inhibits InhA, the FabI enoyl reductase (ENR) in the fatty acid synthesis (FAS-II) pathway.

The activated form of INH later reacts with NAD^+ to form INH-NAD adduct (17–21). Mutations in KatG, in significant number of the strains make them resistant to INH (22–25). Therefore, the discovery of an InhA inhibitor which can avoid this initial activation step should be effective against INH resistant strains of Mycobacterium tuberculosis (MTB).

Materials and methods:

Dataset and molecular modeling

A dataset of 46 Pyrrolidine carboxamide analogues reported to have Enoyl acyl carrier protein reductase inhibitory activities (26) were used for the following QSAR studies (Table 1). In vitro inhibitory concentrations (IC_{50}) of the molecules against Enoyl acyl carrier protein reductase were converted into corresponding pIC_{50} values and used as dependent variables in the 3D-QSAR calculations.

All the molecules were divided into two training sets (30 compounds) for generating 3D-QSAR models and a test set (16 compounds respectively) for validating the quality of the models. The test set was selected based on the criteria given by Oprea et al (27).

All molecular studies were performed using the molecular modeling package SYBYL 6.7.1 (28) on silicon graphics work-station. Energy minimization was performed in SYBYL using Tripos force field (29). The conformations were generated for the most active compounds 41. As the compound is relatively rigid we have used systematic search method with a step size of 158 torsion angle to generate the conformational model. The lowest energy conformer was selected and further geometry optimization of each molecule was carried out with MOPAC 6 package using the semi-empirical AM1 Hamiltonian (20). Optimized structures with MOPAC charges were used for subsequent calculations. This conformer was considered for the building of other molecules.

Alignment

In the standard CoMFA procedure, bioactive conformations are desired for superimposing ligand. In the absence of available crystallographic data information on Enoyl acyl carrier protein reductase and inhibitor complexes, we assumed that the active conformer corresponds to the lowest energy conformer of the conformational model. The molecular alignment was done with the atom-based RMS fit method using the command ALIGN DATABASE present in SYBYL.

This option aligns the structures by pair-wise atom super positioning and all structures in the database are arranged with the same frame of reference as the template compound. The most active compound 41 was used as template and the remaining molecules were aligned to it through using the basic core of Pyrrolidine carboxamide respectively. The aligned molecules are shown in Fig. 1.

CoMFA interaction energy fields

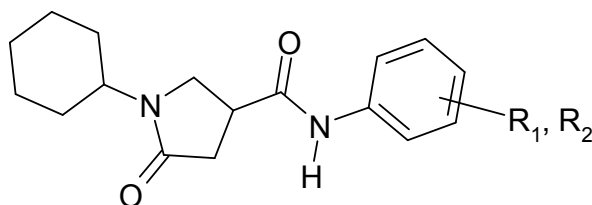
The basic assumption of CoMFA is that compounds having similar pharmacophoric pattern will orient and interact with the receptor/enzyme in similar fashion. To mimic such interactions, a 3-D grid box was put around the molecules taken for the study and CoMFA interaction fields were calculated at each lattice intersection of a regularly spaced grid of 2.0 Å by employing Lennard-Jones and Coulomb potentials. The CoMFA fields, depicting the steric and electrostatic interaction with an sp³ carbon atom with +1.0 charge as the probe were calculated using Tripos force field. The steric and electrostatic fields were truncated at ± 30.0 kcal/mol and the electrostatic fields were ignored at points with maximal steric interactions.

PLS analysis

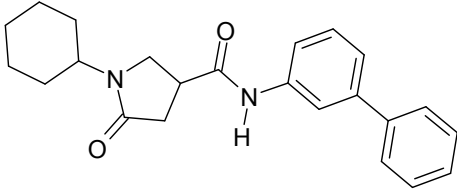
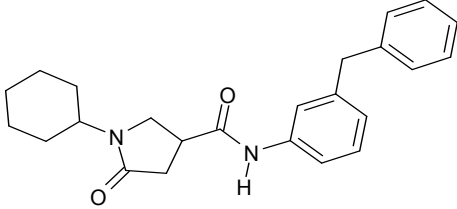
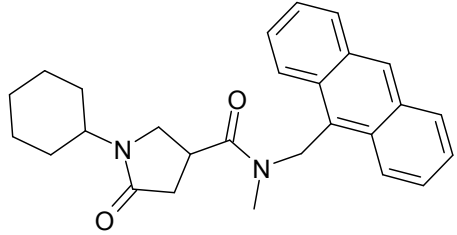
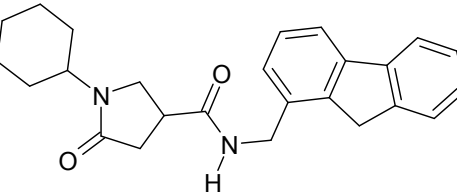
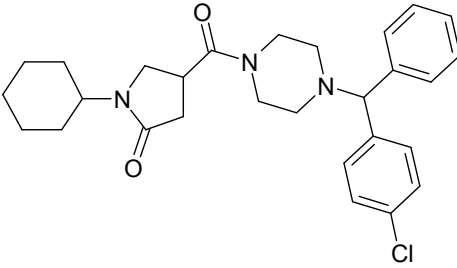
The regression analysis of CoMFA field energies was performed using the partial least squares (PLS) algorithm with the leave-one-out (LOO) method adopted for cross validation. The optimum number of components to be used in conventional analyses was chosen from (i) the analysis with the highest cross validated r² value, and (ii) the model with the smallest standard error of prediction for component models with identical r² values. The column filtering value was set to 2.0 for cross validated runs. Equal weightage was assigned to steric and electrostatic fields. Final analysis was carried out to calculate the conventional r² value using the optimum number of components.

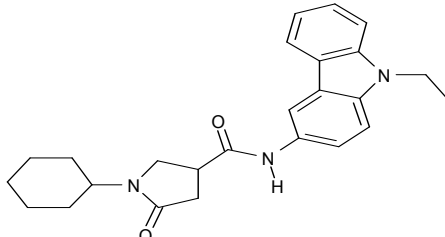
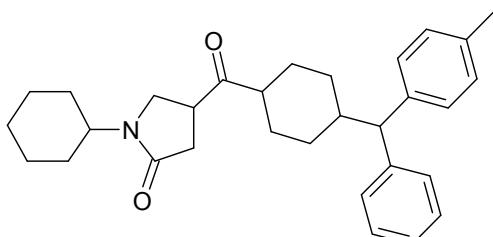
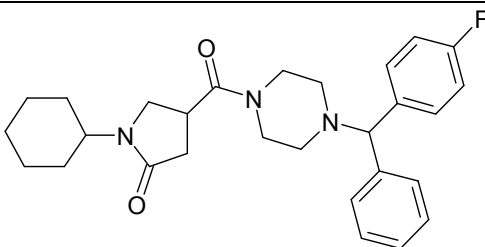
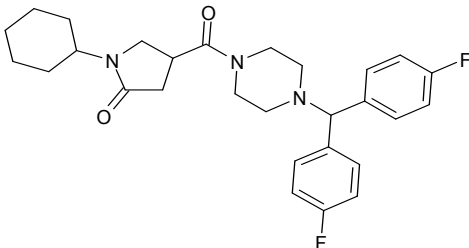
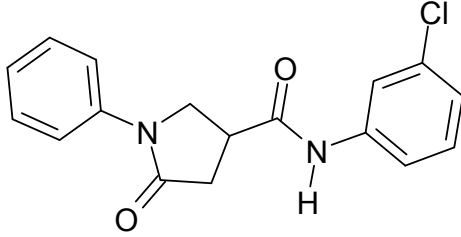
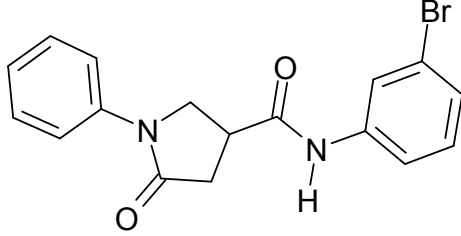
Table 1 : 46 molecules

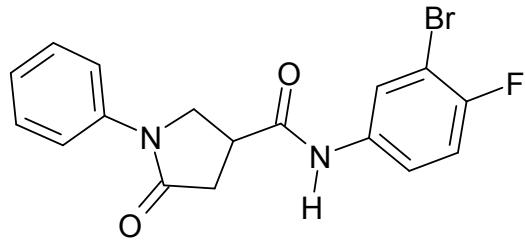
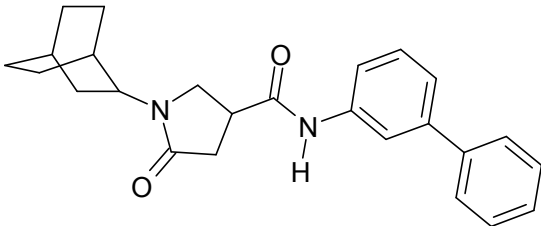
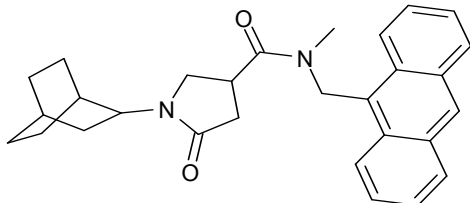
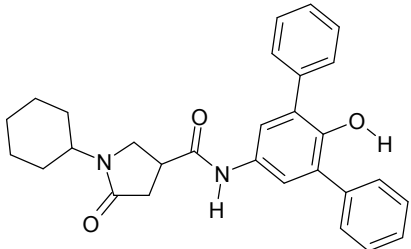
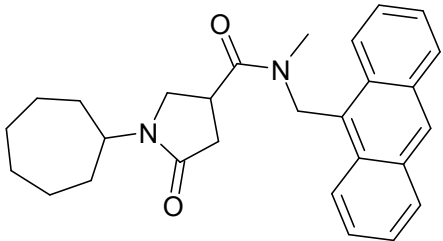
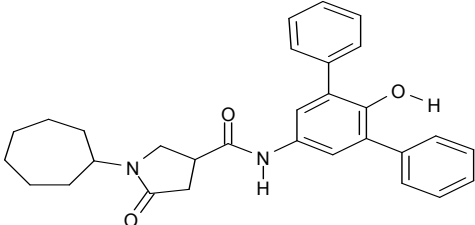
Structures and activities of the molecules



Compound	R1	R2	IC50 [uM]	pIC50 [uM]
1	H	H	10.66	4.972
2	H	2-COOMe	34.88	4.457
3	H	2-Br	0.89	6.051
4	H	3-Br	28.02	4.553
5	H	4-Br	1.35	5.870
6	H	4-I	14.5	4.839
7	H	3-Me	16.79	4.775
8	H	3-CF3	3.51	5.455
9	H	3-NO2	10.59	4.975
10	H	3-CH2[CH3]2	5.55	5.256
11	H	4-Ac	73.58	4.133
12	2-Cl	4-Cl	56.02	4.252
13	2-Cl	5-Cl	56.5	4.248
14	2-Me	5-Cl	0.97	6.013
15	3-Me	4-Br	37.41	4.427
16	2-Me	5-Me	10.05	4.998
17	3-Me	5-Me	3.14	5.503
18	2-Me	3-Cl	23.12	4.636
19	2-Me	4-NO2	31.37	4.503
20	3-F	5-F	1.49	5.827

21	3-Cl	5-Cl	0.39	6.409
22	3-Br	5-CF ₃	0.85	6.071
23	3-OMe	5-CF ₃	1.3	5.886
24	3-CF ₃	5-CF ₃	3.67	5.435
25	2-OMe	5-Cl	1.6	5.796
26	3-Cl	4-F	14.83	4.829
27			0.39	6.409
28			0.41	6.387
29			0.75	6.125
30			1.39	5.857
31			3.39	5.470

32			2.57	5.590
33			2.57	5.590
34			6.41	5.193
35			5.51	5.259
36			3.94	5.405
37			13.55	4.868

38			29.23	4.534
39			0.845	6.073
40			0.46	6.337
41			0.14	6.854
42			0.62	6.208
43			0.36	6.444

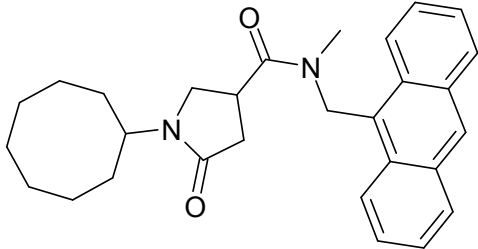
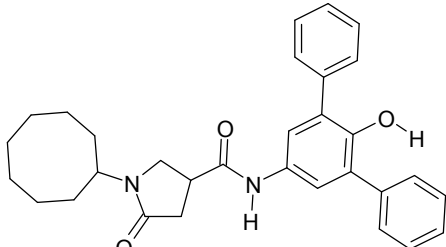
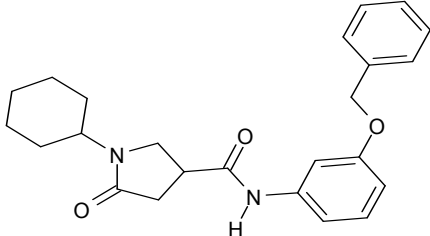
44		0.32	6.495
45		1.29	5.889
46		3.39	5.470

Table 2

CoMFA PLS Result Summary									
q ²	r ²	r ² _{pred}	LOO	LMO	n	F value	SEE	Steric	Electrostatic
0.718	0.966	0.893	0.777	0.751	5	135.847	0.148	0.484	0.516

Table 3:

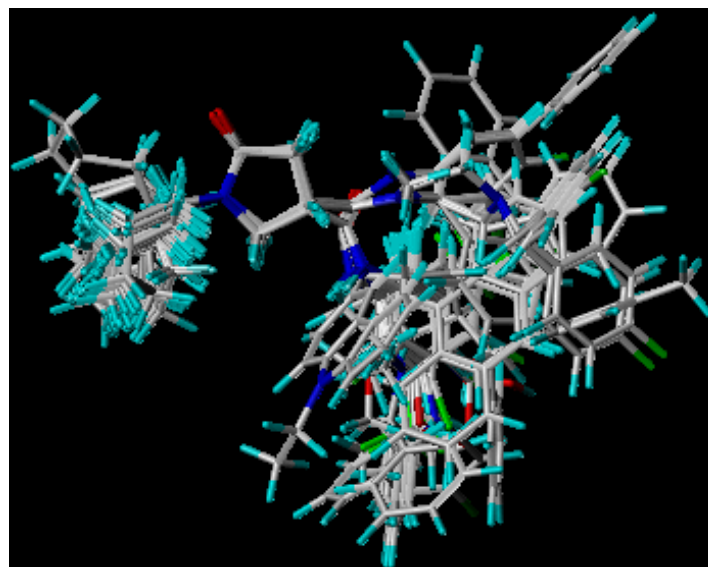
Activities and residuals of training set for CoMFA models

Compound	Actual	Predicted	Residual
2	5.454	5.37	0.084
9	4.975	5.245	-0.27
11	4.133	4.514	-0.381
37	4.868	4.723	0.145
3	6.05	5.598	0.452
38	4.534	4.775	-0.241
6	4.838	4.958	-0.12
12	4.251	4.955	-0.704
20	5.826	5.542	0.284
21	6.408	5.865	0.543
22	6.07	6.202	-0.132
23	5.886	6.056	-0.17
25	5.795	5.449	0.346
17	5.503	5.695	-0.192
18	4.636	5.439	-0.803
19	4.503	4.58	-0.077
29	6.124	5.845	0.279
28	6.387	6.355	0.032
27	6.408	6.289	0.119
33	5.285	5.273	0.012
34	5.193	5.438	-0.245
30	5.856	5.56	0.296
32	5.59	5.445	0.145
35	5.258	5.23	0.028
39	6.073	5.265	0.808
40	6.337	5.683	0.654
41	6.853	6.298	0.555
42	6.443	6.416	0.027
43	5.889	6.522	-0.633
1	4.972	5.202	-0.23

Table 4: Activities and residuals of test set for CoMFA models

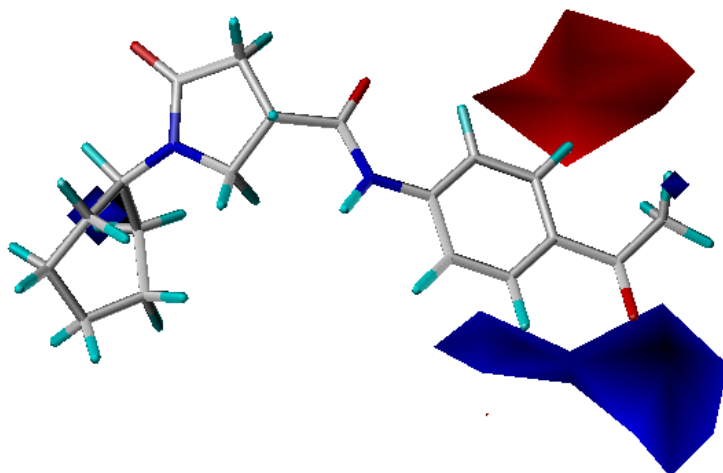
Compound	pIC50	CoMFA	
		Predicted	Residual
36	5.404	4.85	0.554
24	5.435	5.727	-0.835
26	4.828	5.11	-0.782
14	6.013	5.838	0.775
15	4.427	4.422	-0.995
16	4.997	5.121	-0.424
31	5.349	5.753	-0.404
7	4.774	4.877	-1.103
10	5.255	5.942	-0.787
4	4.552	4.85	-0.998
5	5.869	5.673	0.696
13	4.248	4.325	-0.077
42	6.208	5.913	0.295
46	5.47	6.057	-0.587
2	4.457	4.730	-0.273

Fig 1: Alignment of 46 molecules

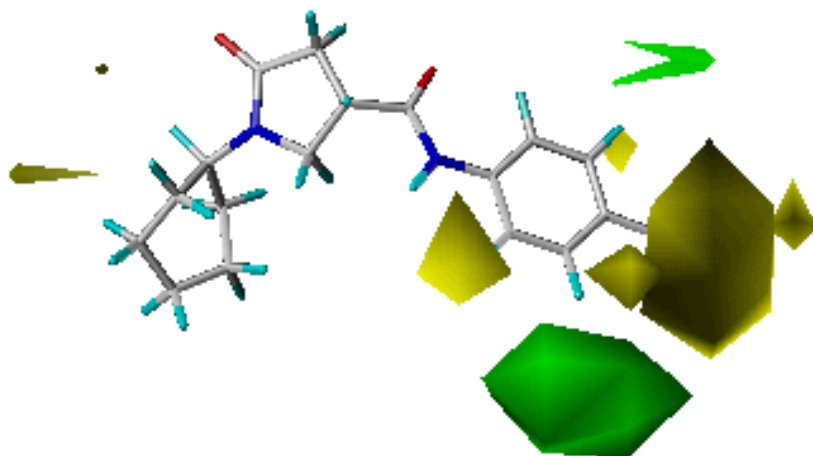


Contour Maps:

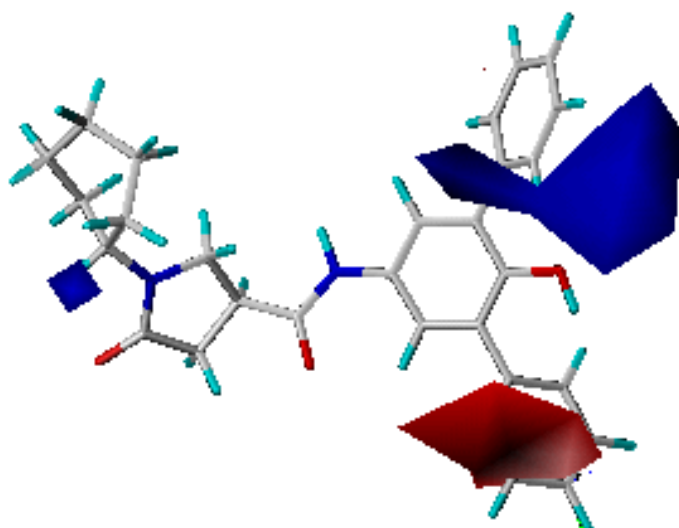
- 1) Electrostatic contour maps of least active compound 11



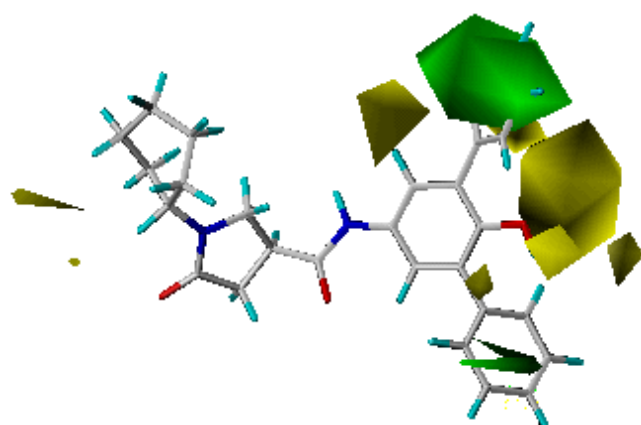
2) Steric contour maps of least active compound 11



3) Electrostatic contour maps of most active compound 41



4) Steric contour maps of most active compound 41



Results and discussion

The predictive 3D-QSAR models were generated for the training sets of Enoyl acyl carrier protein reductase inhibitors using default parameters of COMFA, as determined by cross validation. Reliability of the QSAR models was statistically validated using several statistical parameters, such as r^2 , q^2 and r^2 pred. A total of 46 compounds were partitioned into a training set of 30 and a test set of 16 compounds at random. Bias was given to both structural and biological diversity in both the sets. Table 3 and 4 lists the experimental activities, predicted activities and residual values of the training set and test set by CoMFA model. The CoMFA models yielded a good cross-validated correlation coefficient with LOO of 0.777 and with leave-many-out (q^2 with 10 groups) was 0.751, thus the predictions obtained with these models were reliable. These internal validation methods (leave-one-out and leave-one-out) determine the stability of the developed models.

The non-cross-validated PLS analysis evaluated the correlation coefficient value (r^2) as 0.966 and the standard error of estimate (SEE) was observed as 0.148. F-value stands for the degree of statistical confidence on the developed models and the model has good value of 135.847. The statistical data obtained from the standard CoMFA model constructed with steric and electrostatic fields are depicted in Table 2. The steric and electrostatic contributions are 48.4% and 51.6%, respectively.

Conclusions

In the current study, we have successfully established the ligand-based 3D QSAR CoMFA model on 46 Pyrrolidine carboxamide derivatives, reported as enoyl acyl carrier protein reductase inhibitors. This model has good statistical results in terms of q^2 and r^2 values and showed a great predictivity of the test set, in the external validation, without visible outliers. The model gave q^2 and r^2 values of 0.718 and 0.966. The CoMFA results suggest that steric interactions (48.4%) as well as electrostatic interactions (51.6%) contribute to the activities of inhibitors. The effect of steric and electrostatic fields around aligned molecules was clarified by analyzing CoMFA contour maps. This comparative analysis of contour maps is expected to be of an aid in the design of compounds with an enhanced inhibitory activity and better selectivity to enoyl acyl carrier protein reductase.

References

1. WHO Report, 2007, <www.who.int/tb/publications/global_report/2007/pdf/full.pdf>.
2. Aziz, M. A.; Wright, A.; Laszlo, A.; De Muynck, A.; Portaels, F.; Van Deun, A.; Wells, C.; Nunn, P.; Blanc, L. Epidemiology of antituberculosis drug resistance (the Global Project on Anti-tuberculosis Drug Resistance Surveillance): an updated analysis *M. Lancet* 2006; 368: 2142-54
3. Raviglione, M. C.; Smith, I. M. N. Engl. XDR Tuberculosis — Implications for Global Public Health *J. Med.* 2007; 356: 656-659
4. Pasqualoto, K. F.; Ferreira, E. I.; Santos-Filho, O. A.; Hopfinger, A. J. Rational design of new antituberculosis agents: receptor-independent four-dimensional quantitative structure-activity relationship analysis of a set of isoniazid derivatives *J Med Chem.* 2004 Jul 15;47(15):3755-64.
5. Wei, C. J.; Lei, B.; Musser, J. M.; Tu, S. C. Isoniazid Activation Defects in Recombinant *Mycobacterium tuberculosis* Catalase-Peroxidase (KatG) Mutants Evident in InhA Inhibitor Production *Antimicrob. Agents Chemother.* 2003; 47: 670-675
6. Morlock, G. P.; Metchock, B.; Sikes, D.; Crawford, J. T.; Cooksey, R. C. ethA, inhA, and katG Loci of Ethionamide-Resistant Clinical *Mycobacterium tuberculosis* Isolates *Antimicrob. Agents Chemother.* 2003; 47: 3799-3805.
7. Ormerod, L. P. Multidrug-resistant tuberculosis (MDR-TB): epidemiology, prevention and treatment *Br Med Bull* 2005; 73-74: 17-24.
8. Zhao, X.; Yu, S.; Magliozzo, R. S. Characterization of the binding of isoniazid and analogues to *Mycobacterium tuberculosis* catalase-peroxidase *Biochemistry* 2007; 46: 3161-70.
9. Rawat, R.; Whitty, A.; Tonge, P. J. The isoniazid-NAD adduct is a slow, tight-binding inhibitor of InhA, the *Mycobacterium tuberculosis* enoyl reductase: adduct affinity and drug resistance *Proc. Natl. Acad. Sci. USA* 2003; 100(24), 13881-6.
10. Schaeffer, M. L.; Agnihotri, G.; Volker, C.; Kallender, H.; Brennan, P. J.; Lonsdale, J. T. Purification and biochemical characterization of the *Mycobacterium tuberculosis* beta-ketoacyl-acyl carrier protein synthases KasA and KasB *J. Biol. Chem.* 2001; 276: 47029-37.
11. Kuo, M. R.; Morbidoni, H. R.; Alland, D.; Sneddon, S. F.; Gourlie, B. B.; Staveski, M. M.; Leonard, M.; Gregory, J. S.; Janjigian, A. D.; Yee, C.; Kreiswirth, B.; Iwamoto, H.; Perozzo, R.; Jacobs, W. R., Jr.; Sacchettini, J. C.; Fidock, D. A. Targeting Tuberculosis and Malaria Through Inhibition of Enoyl Reductase: Compound Activity and Structural Data *J. Biol. Chem.* 2003; 278: 20851-59.
12. Choi, K. H.; Kremer, L.; Besra, G. S.; Rock, C. O. Identification and substrate specificity of beta -ketoacyl (acyl carrier protein) synthase III (mtFabH) from *Mycobacterium tuberculosis* *J. Biol. Chem.* 2000; 275: 28201-7.
13. Kremer, L.; Douglas, J. D.; Baulard, A. R.; Guy, M. R.; Morehouse, C.; Alland, D.; Dover, L. G.; Lakey, J. H.; Jacobs, W. R., Jr.; Brennan, P. J.; Minnikin, D. E.; Besra, G. S. Thiolactomycin and Related Analogues as Novel Anti-mycobacterial Agents Targeting KasA and KasB Condensing Enzymes in *Mycobacterium tuberculosis* *J. Biol. Chem.* 2000; 275: 16857-64.
14. Ducasse-Cabanot, S.; Cohen-Gonsaud, M.; Marrakchi, H.; Nguyen, M.; Zerbib, D.; Bernadou, J.; Daffe, M.; Labesse, G.; Quemard, A. In Vitro Inhibition of the *Mycobacterium tuberculosis* β -Ketoacyl-Acyl Carrier Protein Reductase MabA by Isoniazid *Antimicrob. Agents Chemother.* 2004; 48: 242-249.

15. Altered NADH/NAD⁺ Ratio Mediates Coresistance to Isoniazid and Ethionamide in Mycobacteria *Antimicrob. Agents Chemother.* 2005; 49: 708-720.
16. Brennan, P. J.; Rooney, S. A.; Winder, F. G. Ir. The lipids of Mycobacterium tuberculosis BCG: fractionation, composition, turnover and the effects of isoniazid *J. Med. Sci.* 1970; 3: 371-390.
17. Johnsson, K.; King, D. S.; Schultz, P. G. Studies on the mechanism of action of isoniazid and ethionamide in the chemotherapy of tuberculosis *J. Am. Chem.Soc.* 1995; 117: 5009-5010.
18. Marcinkeviciene, J. A.; Magliozzo, R. S.; Blanchard, J. S. Purification and Characterization of the Mycobacterium smegmatis Catalase-Peroxidase Involved in Isoniazid Activation *J. Biol. Chem.* 1995; 270: 22290-22295.
19. Basso, L. A.; Zheng, R. J.; Blanchard, J. S. Kinetics of inactivation of WT and C243S mutant of Mycobacterium tuberculosis enoyl reductase by activated isoniazid. *J. Am. Chem.Soc.* 1996; 118: 11301-2.
20. Quemard, A.; Dessen, A.; Sugantino, M.; Jacobs, W. R., Jr.; Sacchettini, J. C.; Blanchard, J. S. Binding of Catalase-Peroxidase-Activated Isoniazid to Wild-Type and Mutant Mycobacterium tuberculosis Enoyl-ACP Reductases *J. Am. Chem. Soc.* 1996; 118: 1561-1562.
21. Rawat, R.; Whitty, A.; Tonge, P. J. The isoniazid-NAD adduct is a slow, tight-binding inhibitor of InhA, the Mycobacterium tuberculosis enoyl reductase: adduct affinity and drug resistance *Proc. Natl. Acad. Sci.U.S.A.* 2003; 100: 13881-13886.
22. Zhang, Y.; Heym, B.; Allen, B.; Young, D.; Cole, S. The catalase-peroxidase gene and isoniazid resistance of Mycobacterium tuberculosis *Nature* 1992; 358: 591-593.
23. Stoeckle, M. Y.; Guan, L.; Riegler, N.; Weitzman, I.; Kreiswirth, B.; Kornblum, J.; Laraque, F.; Riley, L. W. Catalase-peroxidase gene sequences in isoniazid-sensitive and -resistant strains of Mycobacterium tuberculosis from New York City *J. Infect. Dis.* 1993; 168: 1063-5.
24. Musser, J. M.; Kapur, V.; Williams, D. L.; Kreiswirth, B. N.; van Soolingen, D.; van Embden, J. D. Characterization of the catalase-peroxidase gene (katG) and inhA locus in isoniazid-resistant and -susceptible strains of Mycobacterium tuberculosis by automated DNA sequencing: restricted array of mutations associated with drug resistance *J. Infect. Dis.* 1996; 173: 196-202.
25. Ramaswamy, S. V.; Reich, R.; Dou, S. J.; Jasperse, L.; Pan, X.; Wanger, A.; Quitugua, T.; Graviss, E. A. Single Nucleotide Polymorphisms in Genes Associated with Isoniazid Resistance in Mycobacterium tuberculosis *Antimicrob. Agents Chemother.* 2003; 47: 1241-1250.
26. Xin He; Akram Alian; Robert Stroud; Paul R. Ortiz de Montellano. Pyrrolidine Carboxamides as a Novel Class of Inhibitors of Enoyl Acyl Carrier Protein Reductase from Mycobacterium tuberculosis. *J. Med. Chem.*, 2006, 49 [21], 6308-6323
27. T.I. Oprea; C.L. Waller; G.R. Marshall. Three-dimensional quantitative structure-activity relationship of human immunodeficiency virus (I) protease inhibitors. 2. Predictive power using limited exploration of alternate binding modes. *J. Med. Chem.* 37 [1994] 2206-2215.
28. Sybyl 6.7.1, Tripos Inc., 1699 South Hanley Road, St. Louis, Missouri, 63144, USA.
29. M. Clark; R.D. Cramer III; N.V. Opdenbosch. Validation of the general purpose Tripos 5.2 forcefield. *J. Comput. Chem.* 10 [1989] 982-1012.
30. M.J.S. Dewar; E.G. Zoebisch; E.F. Healy; J.J.P. Stewart. Development and use of quantum mechanical molecular models. 76. AM1: a new general purpose quantum mechanical molecular model. *J. Am. Chem. Soc.* 107 [1985] 3902-3909.